

# High speed spatially multimode atomic memory

T. Golubeva, Yu. Golubev  
*St. Petersburg State University,  
198504 St. Petersburg, Stary Petershof,  
ul. Ul'yanovskaya, 1, Russia*

O. Mishina, A. Bramati, J. Laurat, E. Giacobino  
*Laboratoire Kastler Brossel, Université Pierre et Marie Curie, Ecole Normale Supérieure,  
CNRS, Case 74, 4 place Jussieu, 75252 Paris Cedex 05, France*  
(Dated: February 28, 2011)

We study the coherent storage and retrieval of a very short multimode light pulse in an atomic ensemble. We consider a quantum memory process based on the conversion of a signal pulse into a long-lived spin coherence via light matter interaction in an on-resonant  $\Lambda$ -type system. In order to study the writing and reading processes we analytically solve the partial differential equations describing the evolution of the field and of the atomic coherence in time as well as in space. We show how to optimize the process for writing as well as for reading. If the medium length is fixed, for each length, there is an optimal value of the pulse duration. We discuss the information capacity of this memory scheme and we estimate the number of transverse modes that can be stored as a quantum hologram.

PACS numbers: 42.50.Gy, 42.50.Ct, 32.80.Qk, 03.67.-a

## I. INTRODUCTION

Storage and read out of quantum states of light in matter represent a major challenge for quantum communications and quantum information processing. Since the first proposals for such process about a decade ago [1, 2], and the first experimental implementations [3, 4] a number of schemes have been studied [5, 6]. The main objective is to store and retrieve light pulses or photons without destroying their quantum state, that is the system should be able to store at the same time two on commuting variables like the two quadratures of a light pulses and allow for their retrieval. Mapping quantum states of light like single photons or qubits [7–9], coherent light pulses without noise added [10] and squeezed light [11, 12] onto long lived states of atomic coherence has been first experimentally investigated in alkali-metal gases. More recently quantum memory for entangled photons have been demonstrated in rare-earth doped crystals [13, 14].

While the principle of such memory registers has been mainly developed for a single temporal and spatial mode [15–20], it appears that the need for multiplexing will be high and that multimode memories need to be developed. Several schemes for a spectral multi-mode memory have been proposed based on off resonant Raman interaction [21–23], controlled reversible inhomogeneous broadening (CRIB) [24–27] and atomic frequency comb (AFC) [28], with significant recent experimental advances in vapors [29–32] and crystals [33]. In the direction towards spatial multimode storage of a quantum image, a quantum hologram scheme was proposed in reference [34], based on quantum non demolition measurement (QND) type interaction and in reference [35] based on Raman-type interaction in non-collinear field configuration. Experimentally storage of a classical image was demonstrated

in an atomic vapor based on electromagnetically induced transparency (EIT) type interaction [36]. In this paper, we propose a different storage protocol which significantly combines both spectral and spatial types of multiplexing. Our scheme provides a storage of a quantum image carried by a very short broadband light pulse in an atomic medium. We show that it allows both spectral and spatial multimode storage with a good efficiency.

We consider light storage in a three-level medium in a  $\Lambda$ -configuration, with a strong driving field close to resonance with one of the transitions and a weak signal field close to resonance with the other transition. The two lower levels are assumed to be long-lived, being sublevels of the ground state.

The quantum signals carried by the signal pulse will be stored in the long lived ground state coherence of the atomic ensemble. Contrary to other schemes, based on EIT, we consider very short pulses, actually much shorter than the excited state decay time. Interaction with the medium is then very fast and it does not allow for the build up of EIT. In contrast to echo-type memory, we consider the simultaneous action of both signal and driving fields on the medium.

Storage based on off-resonant Raman interaction was recently proposed and demonstrated for a light pulse much broader than the natural linewidth [23, 30]. The main difference with our protocol is that we propose to explore a resonant interaction and rely on more efficient light-matter coupling. Contrary to CRIB and AFC based schemes our protocol does not deal with an inhomogeneous broadened medium and does not use any rephasing process. However, we will see that the quantum information storage can be quite efficient, in agreement with [16].

The article is organized as follows. In Sec. II the physical model of a 3D-memory process based on the resonant

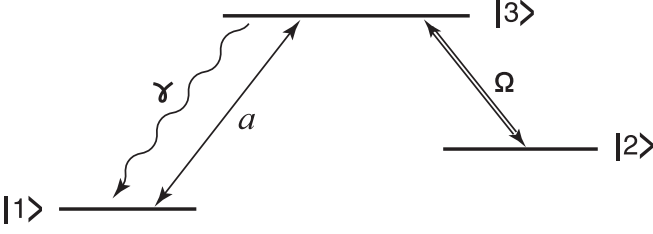


FIG. 1: Three level atomic system interacting with driving field  $\Omega$  and signal field  $a$ .

interaction of the three-level atoms with short pulses is discussed in detail. In Sec. III the writing of a weak quantum field in space and in time is considered. The efficiency and optimization of writing are analyzed. In Sec. IV the read-out is investigated in both forward and backward processes. The role of the diffraction and the number of stored modes are discussed at the end of this section. In App. A the mathematical aspects of the problem are considered in detail.

## II. PHYSICAL MODEL

In this paper, we will study the ability of a system based on ensembles of three-level atoms (Fig. 1) to store temporal as well as spatial multimode quantum fields, thus implementing a quantum hologram. For this, we take the driving field as a plane wave, while the signal field has as a transverse structure. A similar problem has been considered in Ref [34] in the case of a QND interaction of light with atoms.

The signal and driving pulses are assumed to be much shorter than the excited state lifetime  $\gamma^{-1}$ , so that we can neglect spontaneous emission during the writing process, which eliminates a source of fluctuations and dissipation. For the writing process, the driving and signal pulses are assumed to be simultaneous and to have the same duration  $T_W$ . Similarly the driving pulse in the process of read-out has a duration  $T_R$  much smaller than  $\gamma^{-1}$ . Moreover, we assume that duration of the pulses is much larger than the time it takes for the light to go through the atomic medium of length  $L$

$$\gamma^{-1} \gg T_{W,R} \gg L/c. \quad (2.1)$$

The atom-field interaction will be written in the dipole approximation, and the corresponding interaction Hamiltonian reads

$$\hat{V} = - \sum_j \hat{d}_j \hat{E}(\vec{r}_j). \quad (2.2)$$

where  $\vec{r}_j$  represents the spatial coordinates of the  $j$ -th atom and where the field  $\hat{E}(\vec{r}_j)$  is a combination of two fields, signal and driving fields, which are interacting on the two neighboring atomic transitions

$$\hat{E}(\vec{r}, t) = \hat{E}_s(\vec{r}, t) + \hat{E}_d(\vec{r}, t). \quad (2.3)$$

The driving and signal fields are pulses of equal duration that verify Eq.(2.1). The driving field is in a monochromatic coherent state with frequency  $\omega_d$  and propagates as a plane wave with wavevector  $k_d$ . Since most of the atoms are in level  $|1\rangle$ , as explained below, we assume that we can neglect the driving field absorption and that it propagates along the  $z$ -axis through the atomic medium with a constant amplitude  $E_0$ :

$$E_d(\vec{r}, t) = E_0 e^{-i\omega_d t + i k_d z}. \quad (2.4)$$

We treat the signal field in the paraxial approximation as quasi-monochromatic transverse multimode wave of frequency  $\omega_s$  propagating in the same direction as the driving field with an average wavevector  $k_s$ . We can then write the signal field as:

$$\hat{E}_s(\vec{r}, t) = -i \sqrt{\frac{\hbar \omega_s}{2 \epsilon_0 c}} e^{-i\omega_s t + i k_s z} \hat{a}(z, \vec{\rho}, t), \quad (2.5)$$

where  $\hat{a}(z, \vec{\rho}, t)$  is the annihilation operator for the signal field and  $\vec{\rho} = \vec{\rho}(x, y)$  describes the transverse signal field distribution. The amplitude  $\hat{a}(z, \vec{\rho}, t)$  is normalized so that the mean value  $\langle \hat{a}^\dagger(z, \vec{\rho}, t) \hat{a}(z, \vec{\rho}, t) \rangle$  is the photon number per second per unit area.

Using the rotating wave approximation we can write the Hamiltonian as

$$\begin{aligned} \hat{V} = \int dz d^2 \rho \big[ & i \hbar g \hat{a}(z, \vec{\rho}, t) \hat{\sigma}_{31}(z, \vec{\rho}, t) e^{i k_s z} \\ & - i \hbar g \hat{a}^\dagger(z, \vec{\rho}, t) \hat{\sigma}_{13}(z, \vec{\rho}, t) e^{-i k_s z} \\ & + i \hbar \Omega \hat{\sigma}_{32}(z, \vec{\rho}, t) e^{i k_d z} - i \hbar \Omega^* \hat{\sigma}_{23}(z, \vec{\rho}, t) e^{-i k_d z} \big], \end{aligned} \quad (2.6)$$

where  $\hat{\sigma}_{ik}$  are the atomic coherence operators between levels  $i$  and  $k$  and  $d_{ik}$  are the corresponding dipole matrix elements;  $\Omega = E_0 d_{23} / \hbar$  is the Rabi frequency for the driving field ;  $g$  is the coupling constant between the signal field and atom in the dipole approximation:

$$g = \left( \frac{\omega_s}{2 \epsilon_0 \hbar c} \right)^{1/2} d_{31}. \quad (2.7)$$

For the sake of the simplicity we assume  $d_{ik}$  to be real so that  $g = g^*$  and we have set the frequency detunings  $(\omega_s - \omega_{13})$  and  $(\omega_d - \omega_{23})$  equal to zero.

The collective atomic coherences are given by a sum of individual atomic operators

$$\begin{aligned} \hat{\sigma}_{mn}(\vec{r}, t) &= \sum_j |m\rangle \langle n|_j \delta^3(\vec{r} - \vec{r}_j) \\ m, n &= 1, 2, 3, \quad m \neq n, \quad \vec{r} = \{z, \vec{\rho}\}. \end{aligned} \quad (2.8)$$

These operators obey the commutation relation

$$[\hat{\sigma}_{mn}(\vec{r}, t), \hat{\sigma}_{nm}(\vec{r}', t)] = \left( \hat{N}_m(\vec{r}, t) - \hat{N}_n(\vec{r}, t) \right) \delta^3(\vec{r} - \vec{r}'), \quad (2.9)$$

where  $\hat{N}_m$  are the collective atomic population operators

$$\hat{N}_m(\vec{r}, t) = \sum_j |m\rangle \langle m|_j \delta^3(\vec{r} - \vec{r}_j). \quad (2.10)$$

In the paraxial approximation, the slow field amplitude  $\hat{a}(\vec{r}, t)$  obeys the commutation relation

$$[\hat{a}(\vec{r}, t), \hat{a}^\dagger(\vec{r}', t)] = \left(1 - \frac{i}{k_s} \frac{\partial}{\partial z} - \frac{1}{2k_s^2} \frac{\partial^2}{\partial \rho^2}\right) c \delta^3(\vec{r} - \vec{r}'). \quad (2.11)$$

In the following we will assume spatially slowly varying atomic operators and make the substitution

$$\begin{aligned} \hat{\sigma}_{13} &\rightarrow e^{ik_s z} \hat{\sigma}_{13}, \\ \hat{\sigma}_{12} &\rightarrow e^{-i(k_d - k_s)z} \hat{\sigma}_{12}. \end{aligned} \quad (2.12)$$

The driving and signal fields are assumed to be superimposed at all times. They start interacting with the atomic medium at time  $t = 0$ . The input plane of the atomic medium is located at  $z = 0$ . We assume that all the  $N$  atoms are initially in state  $|1\rangle$ .

The complete system of differential equations for the field amplitude and the collective atomic variables is given in Appendix A (A4)-(A10). Here, we will write the evolution equations of the system in the case where the signal field is much weaker than the control field  $|\Omega|^2 \gg g^2 \langle \hat{a}^\dagger \hat{a} \rangle$ . Then most of the atoms remain in ground state  $|1\rangle$  and in the full equation (A6) we can replace the difference of operators  $\hat{N}_1 - \hat{N}_3$  by the c-number  $N$  and we can neglect the term proportional to  $\hat{\sigma}_{23}$ . We only keep the coherences  $\hat{\sigma}_{12}$  and  $\hat{\sigma}_{13}$ . With these approximations, one obtain a simplified system of the form

$$\left( \frac{\partial}{\partial z} - \frac{i}{2k_s} \frac{\partial^2}{\partial \rho^2} \right) \hat{a}(z, \vec{\rho}, t) = -g \hat{\sigma}_{13}(z, \vec{\rho}, t), \quad (2.13)$$

$$\frac{\partial}{\partial t} \hat{\sigma}_{13}(z, \vec{\rho}, t) = gN \hat{a}(z, \vec{\rho}, t) + \Omega \hat{\sigma}_{12}(z, \vec{\rho}, t), \quad (2.14)$$

$$\frac{\partial}{\partial t} \hat{\sigma}_{12}(z, \vec{\rho}, t) = -\Omega^* \hat{\sigma}_{13}(z, \vec{\rho}, t). \quad (2.15)$$

Due to the assumption that the light pulses are much longer than the medium, we have neglected the transient regime associated with the time derivative of the signal field in Eq. (2.13).

We now take the Fourier transform of Eqs. (2.13)-(2.15) as

$$\begin{aligned} \hat{F}(z, t; \vec{q}) &= \frac{1}{2\pi} \int \hat{F}(z, \vec{\rho}, t) e^{-i\vec{q}\vec{\rho}} d^2\rho, \\ \hat{F}(z, \vec{\rho}, t) &= \frac{1}{2\pi} \int \hat{F}(z, t; \vec{q}) e^{i\vec{q}\vec{\rho}} d^2q, \end{aligned} \quad (2.16)$$

and we make the following substitutions

$$\begin{aligned} \hat{a}(z, t; \vec{q}) &\rightarrow \hat{a}(z, t; \vec{q}) e^{-iq^2 z / (2k_s)}, \\ \hat{\sigma}_{mn}(z, t; \vec{q}) &\rightarrow \hat{\sigma}_{mn}(z, t; \vec{q}) e^{-iq^2 z / (2k_s)}. \end{aligned} \quad (2.17)$$

Then the set of partial differential equations giving the evolution of the system reads

$$\frac{\partial}{\partial z} \hat{a}(z, t; \vec{q}) = -g \hat{\sigma}_{13}(z, t; \vec{q}), \quad (2.18)$$

$$\frac{\partial}{\partial t} \hat{\sigma}_{13}(z, t; \vec{q}) = gN \hat{a}(z, t; \vec{q}) + \Omega \hat{\sigma}_{12}(z, t; \vec{q}), \quad (2.19)$$

$$\frac{\partial}{\partial t} \hat{\sigma}_{12}(z, t; \vec{q}) = -\Omega^* \hat{\sigma}_{13}(z, t; \vec{q}). \quad (2.20)$$

These equations are similar to the equations obtained in Refs. [15, 16, 37] for the plane wave case. However, let us underscore that they include the transverse spatial dependence of the signal field and they allow to treat completely the case of a multimode transverse field. Moreover, we present here a full treatment where the hypothesis of very large values of  $|\Omega| \gg g\sqrt{cN}$  is not made.

### III. ANALYSIS OF THE WRITING PROCESS

#### A. Semiclassical solutions of the equations for the writing process

The aim of this section is to derive exact solutions for the system of equations (2.18) - (2.20), in order to have a detailed information on the efficiency of the writing and reading processes in the atomic medium in various conditions. This will allow optimizing the storage and retrieval processes. In order to solve these equations, we will use the Laplace transformation in the time domain [16, 38]. In this case two of the three differential equations are transformed into linear algebraic equations, and the solution of the third differential equation can be written in an explicit form. An inverse Laplace transform then gives the values of the amplitude  $\hat{a}(z, t; \vec{q})$  and coherences  $\hat{\sigma}_{12}(z, t; \vec{q})$  and  $\hat{\sigma}_{13}(z, t; \vec{q})$  under arbitrary initial conditions. The detailed description can be found in Appendix A. In the following we will concentrate on the efficiency of our memory model, for which the semiclassical solutions are sufficient [15, 16].

According to Appendix A the semiclassical solutions for the writing stage for arbitrary relations between  $g^2 cN$  and  $|\Omega|^2$  read

$$a^W(t, z; \vec{q}) = \int_0^t dt' a_{in}(t'; \vec{q}) D(t - t', z), \quad (3.1)$$

$$\sigma_{12}^W(t, z; \vec{q}) = -gN \int_0^t dt' \sin |\Omega|(t - t') \int_0^{t'} dt'' a_{in}(t''; \vec{q}) D(t' - t'', z), \quad (3.2)$$

$$\sigma_{13}^W(t, z; \vec{q}) = gN \int_0^t dt' \cos |\Omega|(t - t') \int_0^{t'} dt'' a_{in}(t''; \vec{q}) D(t' - t'', z), \quad (3.3)$$

where the kernel  $D(z, t)$  is expressed via the first-order Bessel function of the first kind  $J_1$  in the form

$$D(z, t) = \delta(t) - \cos |\Omega|t \sqrt{\frac{2g^2 N z}{t}} J_1 \left( \sqrt{2g^2 N z t} \right) + \frac{1}{2} g^2 N z \int_0^t dt' \left[ \frac{1}{\sqrt{t'}} e^{-i|\Omega|t'} J_1 \left( \sqrt{2g^2 N z t'} \right) \right] \left[ \frac{1}{\sqrt{t-t'}} e^{i|\Omega|(t-t')} J_1 \left( \sqrt{2g^2 N z (t-t')} \right) \right]. \quad (3.4)$$

To examine the efficiency of the storage for each spatial spectral field component, we assume that an amplitude of the input signal pulse is constant in time,

$$a_{in}(t, \vec{q}) = a_{in}(\vec{q}). \quad (3.5)$$

In view of numerical calculations, the solutions can then be written in the following form

$$a^W(\tilde{t}, \tilde{z}; \vec{q}) = a_{in}(\vec{q}) \left[ 1 + \int_0^{\tilde{t}} d\tilde{t}' \tilde{D}(\tilde{t}', \tilde{z}) \right], \quad (3.6)$$

$$\sigma_{12}^W(\tilde{t}, \tilde{z}; \vec{q}) = -p a_{in}(\vec{q}) \left[ 1 - \cos \tilde{t} + \int_0^{\tilde{t}} d\tilde{t}' [1 - \cos(\tilde{t} - \tilde{t}')] \tilde{D}(\tilde{t}', \tilde{z}) \right], \quad (3.7)$$

$$\sigma_{13}^W(\tilde{t}, \tilde{z}; \vec{q}) = p a_{in}(\vec{q}) \left[ \sin \tilde{t} + \int_0^{\tilde{t}} d\tilde{t}' \sin(\tilde{t} - \tilde{t}') \tilde{D}(\tilde{t}', \tilde{z}) \right], \quad (3.8)$$

where we define a new kernel  $\tilde{D}(\tilde{t}, \tilde{z})$  as

$$D(t, z) = |\Omega| \left[ \delta(\tilde{t}) + \tilde{D}(\tilde{t}, \tilde{z}) \right], \quad (3.9)$$

and

$$\tilde{D}(\tilde{t}, \tilde{z}) = -\cos \tilde{t} \sqrt{\frac{\tilde{z}}{\tilde{t}}} J_1(\sqrt{\tilde{z}\tilde{t}}) + \frac{1}{4} \tilde{z} \int_0^{\tilde{t}} d\tilde{t}' \left[ \frac{1}{\sqrt{\tilde{t}'}} e^{-i\tilde{t}'} J_1(\sqrt{\tilde{z}\tilde{t}'} ) \right] \left[ \frac{1}{\sqrt{\tilde{t}-\tilde{t}'}} e^{i(\tilde{t}-\tilde{t}')} J_1(\sqrt{\tilde{z}(\tilde{t}-\tilde{t}')} ) \right]. \quad (3.10)$$

We have defined an effective interaction coefficient  $p$ , given by

$$p = \frac{gN}{|\Omega|}$$

and we have introduced dimensionless values of for time  $\tilde{t}$  and space  $\tilde{z}$ , defined by

$$\tilde{t} = |\Omega| t, \quad \tilde{z} = \frac{2g^2 N}{|\Omega|} z. \quad (3.11)$$

The above definitions can be understood in the following way. We focus our analysis on a time scale on which the

spontaneous decay of the upper level is negligible, so the effective evolution rate of the levels is determined by the Rabi frequency  $\Omega$ . The inverse Rabi frequency  $\Omega^{-1}$  is then the natural time unit. Moreover, if we replace the relaxation constant of the upper level  $\gamma$  by an effective decay rate which is the Rabi frequency in the usual expression of the optical depth for an atomic medium of length  $z$ , we get an effective optical depth  $2g^2 N z / |\Omega|$ . This expression is the dimensionless space coordinate  $\tilde{z}$  defined above.

The expression for the probe field amplitude (3.1) is the convolution of the field value at the input of the medium with the kernel  $D(z, t)$ . The expressions for

the coherences (3.2)-(3.3) involve double convolutions. Rather than looking for an analytical solution, we have solved this system numerically, and in the next sections, we analyze the results of this calculation.

### B. Evolution of the signal field and of the atomic coherence inside the memory cell

As stated earlier, we study here the light-matter interface in conditions where the light pulse is much shorter than the atomic excited state lifetime but much longer than its propagation time in the atomic medium  $L/c$ . Thus the propagation time of the pulse wavefronts inside the medium is very short, and we can neglect the evolution of the field and the atomic state and also any energy exchange between field and atoms over times on the order of  $L/c$ . In this approximation, we also consider the driving field as constant during the pulse duration  $T_W$ . Note that the latter approximation is not fundamentally necessary for our calculations but it simplifies the solutions.

In view of the above approximations, we can define the writing process duration as the interval between time  $t = 0$ , when the front part of the pulse goes out of the medium and time  $t = T_W$  when the end of the pulse reaches the input surface of the medium.

Let us normalize the amplitude  $a^W(\tilde{t}, \tilde{z}, \vec{q})$  of the input field with respect to its value before it enters the medium, and the coherence  $\sigma_{12}^W(\tilde{t}, \tilde{z}, \vec{q})$  with respect to its maximal possible value at point  $\tilde{z} = 0$ , which can be shown to be  $-2pa_{in}(\vec{q})$  as  $\tilde{t} = \pi$  from Eqs. (3.6)-(3.7). The normalized signal field and atomic coherence can be written as

$$\begin{aligned} a^W(\tilde{t}, \tilde{z}) &= \frac{a^W(\tilde{t}, \tilde{z}, \vec{q})}{a_{in}(\vec{q})}, \\ \sigma_{12}^W(\tilde{t}, \tilde{z}) &= -\frac{\sigma_{12}^W(\tilde{t}, \tilde{z}, \vec{q})}{2pa_{in}(\vec{q})}. \end{aligned} \quad (3.12)$$

We first analyze the distribution of the field amplitude inside the medium as a function of time. At time  $\tilde{t} = 0$  the signal field is distributed homogeneously along the medium and is equal to 1. It remains equal to 1 at the entrance of the medium,  $\tilde{z} = 0$  till the end of the signal pulse at  $\tilde{t} = \tilde{T}_W$ .

The three upper panels (a, b and c) of Fig. 2 show the calculated distribution of field amplitude along  $z$  in the atomic medium for times  $\tilde{t} = 0.5, 1$  and  $\pi$ . The amplitude of the field shows an oscillatory behaviour as a function of  $\tilde{z}$ , the effective optical depth at point  $z$ . This behaviour results from the interplay between the signal field and the atoms interacting with the strong driving field.

Because of the interaction of the atoms with the driving and signal fields a small fraction of the atoms initially placed in state  $|1\rangle$  is transferred to state  $|2\rangle$  and an atomic coherence  $\sigma_{12}(\tilde{t}, \tilde{z})$  is generated between states  $|1\rangle$  and  $|2\rangle$ . The evolution of this coherence is shown in the

three lower panels of Fig. 2. This long-lived coherence is the basic feature of the quantum memory.

The lower panels in Fig. 2 clearly show the build-up of the ground state coherence, which results from the integrated interaction of the atomic medium with the field since the beginning of the pulse. Our calculation allows to follow in detail the build-up of this coherence. Up to  $\tilde{t} = \pi$  (which corresponds to a  $\pi$  driving pulse), the coherence  $\sigma_{12}^W(\tilde{t}, \tilde{z})$  increases dramatically with time up to its maximum value of 1 for small values of  $\tilde{z}$  and stays close to 0 for large values of  $\tilde{z}$  ( $\tilde{z} > 15$ ). Thus only the layers close to the input of the atomic medium are involved in the storage process, while deeper inside of the atomic medium, the coherence remains equal to zero.

For longer time intervals the behaviour of the atomic coherence changes. Figure 3 depicts the evolution of  $\sigma_{12}^W(\tilde{t}, \tilde{z})$  as a function of  $\tilde{t}$  and  $\tilde{z}$ . At times later than  $\tilde{t} = \pi$  the distribution the coherence over the medium changes:  $\sigma_{12}^W$  decreases for small  $\tilde{z}$  and starts to grow for larger values of  $\tilde{z}$ . It can be seen clearly in Fig. 3 that the maximum of  $\sigma_{12}^W$  shifts from  $\tilde{z} = 0$  to non zero values of  $\tilde{z}$ .

Such a behavior is the result of two competing processes: local writing and reading of the signal field. Actually, after time  $\tilde{t} = \pi$ , we can consider that the control field starts to "read" the atomic coherence and writes it back further in the medium. Quantum information is transferred from the input layers to the deeper ones. Eventually, the whole medium is involved in the storage process.

If the duration of the field-medium interaction is increased even further, the maximum of the atomic coherence shifts deeper into the atomic medium, as shown in Fig. 4, for  $\tilde{t} = \pi, 2\pi, 3\pi$  and  $4\pi$ .

Let us note that the behavior of the coherence in a thin layer close to the input is similar to the one predicted in Ref. [15] for the case of a single-mode cavity: the coherence increases from 0 to 1 between times 0 and  $\pi$ , then it decreases from 1 to 0 in the following  $\pi$  interval, etc., that is, the writing and reading processes interchange each other with a period  $\pi$ . However, in our case, this is only true for  $z \simeq 0$ . For other points inside the medium, the behaviour is more complex than this periodic oscillation.

### C. Optimization of the writing process

In the previous section, we have analyzed the writing process, that is the build-up of the ground state coherence in the atomic medium. From the calculated distribution of  $\sigma_{12}^W$ , it can be seen that an efficient writing process, with an effective state exchange between signal field and atomic coherence can only be obtained for a pulse duration larger than  $\pi$ . However, as explained below, the  $\pi$  pulse does not necessarily correspond to the optimal duration because it only ensures an effective excitation of the input layers. In order to quantify the

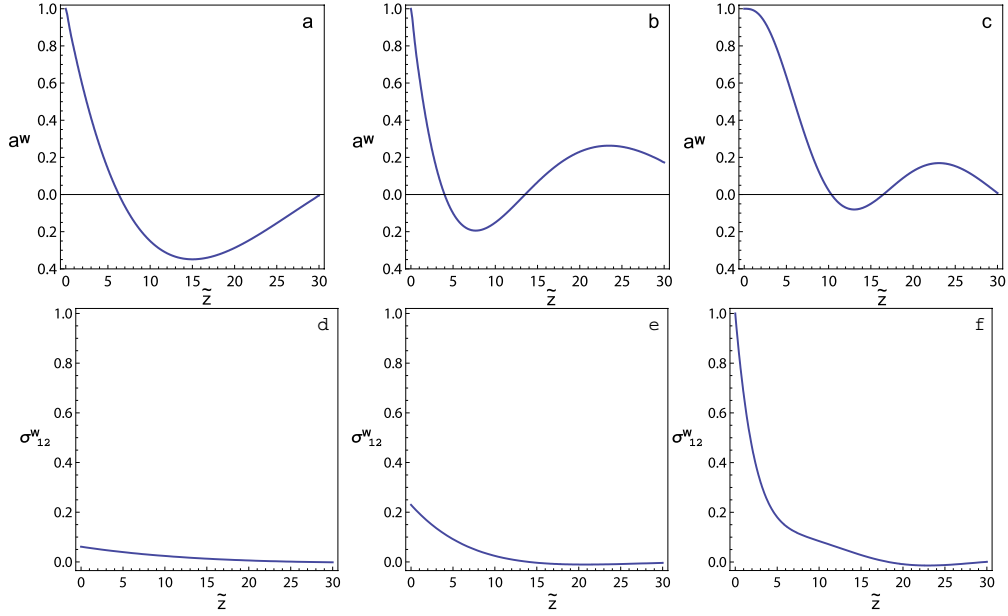


FIG. 2: Normalized distributions of the field amplitude and of the atomic coherence inside the medium at times (a)  $\tilde{t} = 0.5$ ; (b)  $\tilde{t} = 1$ ; (c)  $\tilde{t} = \pi$ .

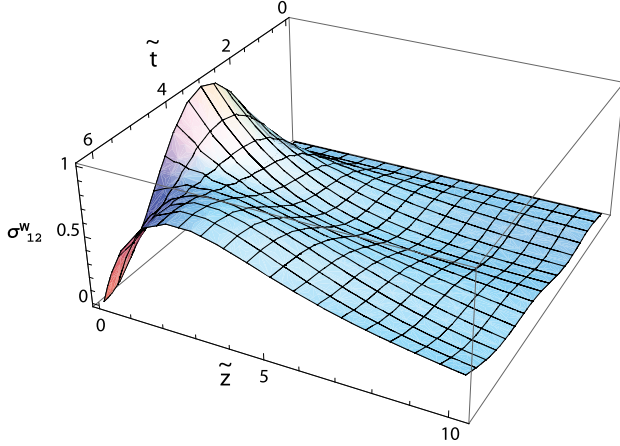


FIG. 3: Distribution of the coherence  $\sigma_{12}^W(\tilde{t}, \tilde{z})$  in time and space.

writing efficiency, we will use the intensity of the outgoing signal field, since any photon from the signal field going out of the medium can be considered as a loss. Using the method presented in the previous section, we obtain the signal field at the output of the medium of length  $\tilde{L}$ ,  $a^W(\tilde{t}, \tilde{L})$ . The time dependence of this field normalized according Eq. (3.12) is shown in Fig. 5 for a specific length of the medium. It can be seen that this outgoing field, usually called leakage may take non negligible values. We will characterize the efficiency of the

memory by the total losses

$$Loss(\tilde{T}_W, L) = \frac{\int_0^{\tilde{T}_W} |a^W(\tilde{t}, \tilde{L})|^2 d\tilde{t}}{\int_0^{\tilde{T}_W} |a_{in}(\tilde{t})|^2 d\tilde{t}} \times 100\% \quad (3.13)$$

For a length  $\tilde{L}$  of the medium and a duration  $\tilde{T}_W$  of the writing pulse, the losses correspond to the integral of the signal field intensity over the duration of the writing pulse  $\tilde{T}_W$  normalized to the full pulse energy.

Using Eq. (3.13), we can optimize the writing efficiency by minimizing the losses. This is shown in Fig. 6, where the upper panels depict the losses as a function of the pulse duration for various medium lengths.

Figure 6 shows that for each length, there is an optimal pulse duration that minimizes the losses. For a medium length of  $\tilde{L} = 10.3$ , the minimal losses are obtained for  $\tilde{T}_W = 4.2$  and are about 5.1 %. The losses decrease with longer atomic media, but at the expense of longer writing pulses.

For each of the considered medium lengths, the lower panels of Fig. 6 show the distribution of the atomic ground state coherence corresponding to the optimal writing time  $\tilde{T}_W$ . For short atomic media and pulse time durations, Fig. 6a, losses are significant due to a field-medium interaction that does not last long enough for the build-up of an appreciable atomic coherence. On the other hand, if the pulse duration is longer than optimal for a given medium length, signal field leakage takes place: the atomic coherence starts to be re-read by the control field resulting in a field emission that increases the losses.

The losses  $Loss(\tilde{T}_W, L)$  can also be calculated as a function of the medium length for a fixed pulse duration.

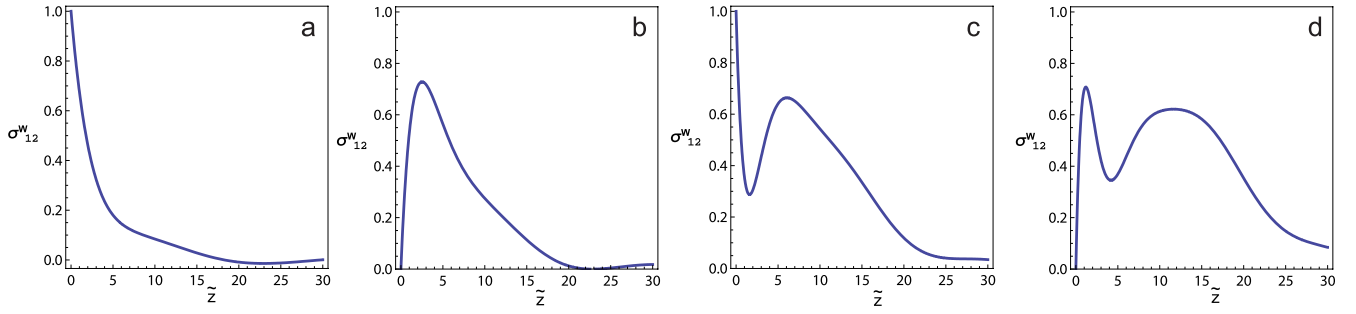


FIG. 4: Distribution of the coherence  $\sigma_{12}^W(\tilde{t}, \tilde{z})$  along the medium for (a)  $\tilde{t} = \pi$ ; (b)  $\tilde{t} = 2\pi$ ; (c)  $\tilde{t} = 3\pi$ ; (d)  $\tilde{t} = 4\pi$ .

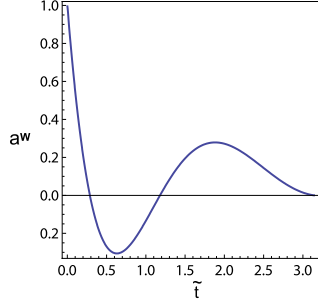


FIG. 5: Field  $a^W(\tilde{t}, \tilde{L})$  at the output of the medium during the writing process for  $\tilde{L} = 10.3$ .

This is shown in Fig. 7. In this case, the losses decrease monotonically when the medium length increases. Thus, if the atomic medium can be considered as an unlimited resource, any signal pulse (satisfying Eq. (2.1)) can be written with a predetermined efficiency. On the other hand, if the length of the medium is limited, then one can no longer write an arbitrary pulse and optimization is required.

Finally let us examine how realistic the parameters requested for optimal writing are. It can be seen in Fig. 6b that the ratio of  $\tilde{L}/\tilde{T}_W$ , ensuring minimum losses is approximately equal to 2.5. Turning back to dimensional variables and separating three main factors, we get

$$\frac{\tilde{L}}{\tilde{T}_W} = \frac{2g^2NL}{\gamma} \frac{1}{\gamma T_W} \frac{\gamma^2}{|\Omega|^2}, \quad (3.14)$$

where  $\gamma$  is the spontaneous decay rate of the upper level. The first factor is the (real) optical depth, that is typically on the order of 1 to 10. The second factor, assuming (2.1) is much larger than 1. Thus, the Rabi frequency is determined by the inequalities  $\gamma^2/|\Omega|^2 \ll 1$ . Also one

can see that these optimal conditions are compatible with  $g\sqrt{Nc} \sim |\Omega|$ . The conditions necessary to reach a good efficiency are expected to be quite feasible.

#### IV. ANALYSIS OF THE READ-OUT PROCESS

##### A. Semiclassical solution of the equations for the read-out process

The quantum information written into the atomic medium as described in the previous section can be stored during a time which is limited by the lifetime of the ground state atomic coherence. For times shorter than this lifetime, the quantum information can be recovered by means of the read-out process. The latter is carried out using a driving pulse at the same frequency as the one in the writing stage. We will consider two possible geometries for the read-out pulse propagation. The first one is the forward retrieval for which the read-out driving pulse propagates in the same direction as the writing pulse. The second one is the backward retrieval for which the read-out pulse has the opposite direction. Like for other memory schemes [18, 39–42], we will see that backward retrieval provides better read-out than forward retrieval for a single mode while it is not necessarily true for a multimode signal.

The solutions of equations (2.18)-(2.20) were obtained in the previous section for specific initial conditions characteristic of the writing process. For read-out it is assumed that the signal field at the input of the medium  $\hat{a}^R(t, z=0; \vec{q})$  and the coherence at the initial time  $\hat{\sigma}_{13}^R(t=0, z; \vec{q})$  are in the vacuum state, i.e., equal to zero in the semiclassical approach. The ground state coherence  $\hat{\sigma}_{12}^R(t=0, z; \vec{q})$  is assumed to coincide with its value at the end of writing stage. First in the case of forward read-out, the solutions describing the reading process are given by (see Appendix A)

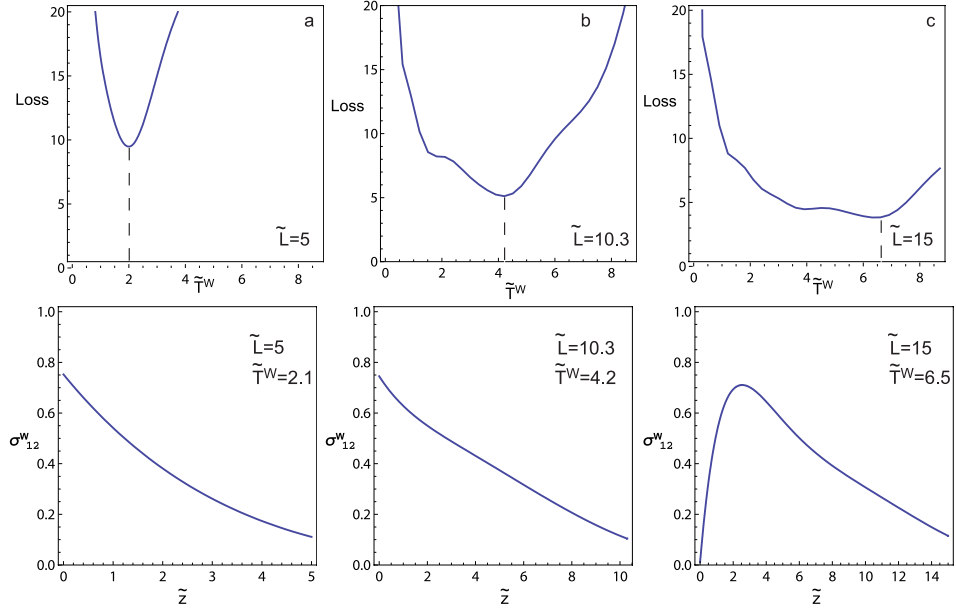


FIG. 6: Writing process : relative losses in the field intensity (in percent of the input field intensity) at the output of the medium as a function of  $\tilde{T}_W$  for (a)  $\tilde{L} = 5$ ; (b)  $\tilde{L} = 10.3$ ; (c)  $\tilde{L} = 15$  and corresponding coherence distribution for optimal conditions.

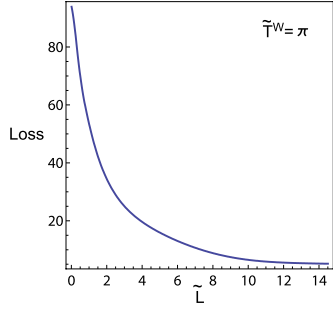


FIG. 7: Writing process : relative losses in the field intensity (in percent of the input field intensity) at the output of the medium as a function of  $\tilde{L}$  for  $\tilde{T}_W = \pi$ .

$$a^R(t, z; \vec{q}) = -g \int_0^z dz' \int_0^t dt' \sin |\Omega| t' \sigma_{12}^W(T_W, z'; \vec{q}) D(t - t', z - z'), \quad (4.1)$$

$$\begin{aligned} \sigma_{13}^R(t, z; \vec{q}) = & \sin |\Omega| t \sigma_{12}^W(T_W, z; \vec{q}) - \\ & - g^2 N \int_0^t dt' \cos |\Omega| (t - t') \int_0^{t'} dt'' \sin |\Omega| t'' \int_0^z dz' \sigma_{12}^W(T_W, z'; \vec{q}) D(t' - t'', z - z'), \end{aligned} \quad (4.2)$$

$$\begin{aligned} \sigma_{12}^R(t, z; \vec{q}) = & \cos |\Omega| t \sigma_{12}^W(T, z; \vec{q}) + \\ & + g^2 N \int_0^t dt' \sin |\Omega| (t - t') \int_0^{t'} dt'' \sin |\Omega| t'' \int_0^z dz' \sigma_{12}^W(T_W, z'; \vec{q}) D(t' - t'', z - z'), \end{aligned} \quad (4.3)$$

where the ground state coherence at the beginning of the process  $\sigma_{12}^W(T_W, z'; \vec{q})$  contains the stored signal field. This value coincides with equation (3.2) at  $t = T_W$ .

Solutions for the backward read-out are similar except for the spatial argument in the coherence  $\sigma_{12}^W(T_W, z'; \vec{q})$  where  $z'$  has to be changed to  $L - z'$ . Substituting the



coherence  $\sigma_{12}$  from Eq.(3.2) to Eq.(4.1) and taking into account the diffraction factors (2.17) one can derive the signal field at the output of the memory cell for the forward read-out of the form

$$a_{forward}^R(\tilde{t}, \tilde{L}; \vec{q}) = \frac{1}{2} a_{in}(\vec{q}) e^{-iq^2 L/(2k_s)} \int_0^{\tilde{L}} d\tilde{z}' \left[ \sin \tilde{t} + \int_0^{\tilde{t}} d\tilde{t}' \sin \tilde{t}' \tilde{D}(\tilde{t} - \tilde{t}', \tilde{L} - \tilde{z}') \right] \times \left[ 1 - \cos \tilde{T}_W + \int_0^{\tilde{T}_W} d\tilde{t}'' [1 - \cos(\tilde{T}_W - \tilde{t}'')] \tilde{D}(\tilde{t}'', \tilde{z}') \right] \quad (4.4)$$

and correspondingly for the backward read-out:

$$a_{back}^R(\tilde{t}, \tilde{L}; \vec{q}) = \frac{1}{2} a_{in}(\vec{q}) \int_0^{\tilde{L}} d\tilde{z}' e^{-iq^2 z'/k_s} \left[ \sin \tilde{t} + \int_0^{\tilde{t}} d\tilde{t}' \sin \tilde{t}' \tilde{D}(\tilde{t} - \tilde{t}', \tilde{z}') \right] \times \left[ 1 - \cos \tilde{T}_W + \int_0^{\tilde{T}_W} d\tilde{t}'' [1 - \cos(\tilde{T}_W - \tilde{t}'')] \tilde{D}(\tilde{t}'', \tilde{z}') \right]. \quad (4.5)$$

These equations are written using the dimensionless time and space coordinates except for the exponential diffraction factor where the regular  $z$  coordinate is kept. One can see that the situation is very different for forward and backward retrieval. For forward read-out the diffraction introduces a common factor which can easily be compensated with an appropriate lens. Thus, in this case, although diffraction takes place separately in writing and reading, the effects of diffraction due to the writing process can be perfectly compensated under the read-out.

A dramatically different situation takes place for the backward read-out. Because the diffraction factor is under the integral, the diffraction are able to modify seriously the initial transverse distribution. In contrast to the first case, the diffraction processes in the writing and reading channels do not compensate each other but on the contrary add their effects. From Eqs. (4.4)-(4.5), it can be seen that under the geometrical conditions  $q^2 L/k_s \ll 1$ , diffraction is not detrimental (see also below). Here we shall consider only this case and we show in Fig. 8 the time dependence of the intensity of the read-out signal.

## B. Efficiency of the memory process

Fig. 8 shows the intensity of the re-emitted normalized signal field  $a^R(\tilde{t}, \tilde{L}) = a^R(\tilde{t}, \tilde{L}, \vec{q})/a_{in}(\vec{q})$  at the output of the medium as a function of the reading time for forward and backward retrieval for an optical depth  $\tilde{L} = 10.3$  and a writing time duration  $\tilde{T}_W = 4.2$ . It can be seen that the shape of the restored pulse is quite different from the shape of the input signal pulse. However, we will not

focus on restoring the pulse shape, but rather, on the read-out of an image corresponding to an ensemble of the transverse modes of the signal field, which has been stored in the atomic medium as a quantum hologram. To do this, the photon number in each of the reconstructed transverse modes must be the same as the photon number in the corresponding modes of the original field. To estimate the storage efficiency, we introduce the parameter  $Eff(\vec{q})$ , defined as the ratio of the integrated intensity of the recovered pulse in mode  $\vec{q}$  to the integrated intensity of the same transverse mode in the input pulse :

$$Eff(\vec{q}) = \frac{\int_0^{\tilde{T}_R} |a^R(\tilde{t}, \tilde{z}, \vec{q})|^2 d\tilde{t}}{\int_0^{\tilde{T}_W} |a_{in}(\tilde{t}, \vec{q})|^2 d\tilde{t}} \times 100\% \quad (4.6)$$

where  $T_R$  is the reading time duration. It can be seen from Fig. 8 that for an efficient recovery, for forward retrieval, the reading time duration should substantially exceed the writing time duration. For example, in Fig. 8a, the retrieval efficiency after a reading time equal to the writing time  $T_W$  is only 36%. For backward retrieval, the retrieval is much more efficient. In Fig. 8b the efficiency reaches 80% for a reading time  $T_R = T_W$ .

Losses come from both the writing and the reading processes. With parameters  $\tilde{L} = 10.3$  and  $\tilde{T}_W = 4.2$  Fig. 6 shows that the losses in the writing process are 5.1%. Then, the best efficiency of the whole process, including writing and read-out cannot exceed  $Eff = 94.9\%$ .

For the reading process, a numerical calculation shows that if the reading time is 10 times the writing time  $T_R = 10T_W$ , the overall efficiency is  $Eff = 77\%$  for forward retrieval. We could choose an even longer reading duration, but we must remain in the approximation that  $T_R \ll \gamma^{-1}$ . The backward retrieval is faster and the same calculation yields an overall efficiency of 83.8% for  $T_R = 3T_W$ .

In the same way as for writing, we observe oscillations in the read-out field in forward direction (Fig. 8a). This indicates that the reading process is accompanied by a rewriting process in the medium, before emission. In the case of backward retrieval, the situation is much more favorable and the curve does not show any oscillation (Fig. 8b).

The read-out as well as the writing is coupled with a displacement of the coherence along the medium. From the results obtained in the previous section it can be seen that for not too long writing pulses, the storage in the atomic coherence is mainly localized in the input layers of the medium. Then, if the medium is long enough, the forward retrieval involves reading the signal and writing it again on successive layers in the medium, which eventually "pushes" the read-out signal out of the medium. On the contrary, in the backward retrieval there is less "pushing", since a large coherence is concentrated at the exit face.

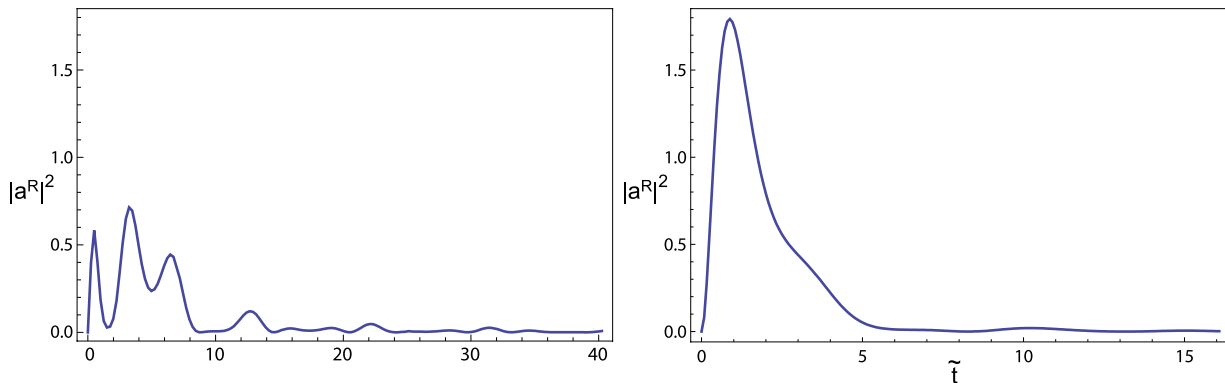


FIG. 8: Reading process : field intensity  $|a^R(\tilde{t}, \tilde{L})|^2$  at the output of the medium for  $\tilde{L} = 10.3$  and  $\tilde{T}_W = 4.2$  for (a) forward and (b) backward propagating retrieval.

### C. Restoring the transverse profile

Let us now examine in more details the information about the transverse profile of the field in the reconstructed pulse. Usually, the quantum memory of the pulse implies its longitudinal profile storage. A lot of works devoted to this problem (for example, [? ], [16], [18]) have focused on the determination of eigenfunctions of the system, we will not deal with this issue. Our goal is to restore the transverse profile of the signal field. To achieve a quantum memory we need to ensure high efficiency of reconstruction for each transverse mode. In the previous section, we showed that each of the transverse modes can be recovered with equal efficiency, with a value that depends on the choice of experimental parameters and that can be high enough. However for the quantum storage of the transverse profile we should have not only a high efficiency for each component but also an insensibility to the diffraction phenomena.

In the previous section we showed that the reading conditions are different depending on whether reading is a direct or reverse process. However, this apparent advantage of backward reading is associated with a limitation due to diffraction phenomena. The essential difference between the forward and backward reading is that in the first case, the diffraction distortions that occur during storage are almost entirely compensated under subsequent reading. What is left uncompensated can be easily cleaned, for example, by setting additional lens at the output of the cell.

In the second case, the diffraction distortions that occur sequentially during recording and reading, add to each other, and they have to be minimized independently. It can be seen that this leads to a significant limitation for an important memory parameter, which is the number of modes or the grain of the image that can be efficiently stored in the memory cell. In principle, this number of modes is determined by the ratio between the transverse size of the memory cell  $S$  and the grain size  $d$  of the image at the entrance to the cell and is equal to  $N = S/d^2$ . Minimizing the diffraction means that at the output of

the memory cell of thickness  $L$  the grain size  $D = L\lambda/d$  should coincide with the input grain size  $D = d$ . This means that the number of stored modes  $N$  can not exceed the Fresnel number  $F_N = S/(\lambda L)$ .

So our numerical analysis of backward reading that does not take diffraction into account can be considered as justified, provided that the number of stored modes is below the Fresnel number  $N \leq F_N$ .

Similarly, we can estimate the number  $N$  for forward reading. In this case, as already mentioned, we can generally ignore the diffraction image distortion associated with the intersection of various grains at the cell output. However, we should not allow excessive beam divergence and, as a result of this divergence, light losses due to leakage of the field through the side walls of the cell. To avoid these losses, the output grain size should not exceed the transverse size of the memory cell  $D \leq \sqrt{S}$ . It is easy to see that the number of stored modes should not exceed the square of the Fresnel number  $N \leq F_N^2$ , in agreement with Ref.[35]. We can thus predict a large storage capacity for this  $\Lambda$ -based memory scheme.

## V. CONCLUSION

We have presented a full calculation of the writing and read-out processes of a short pulse in an atomic medium. Our approach relies on a full treatment of light matter interaction as the writing or reading pulses propagate through the atomic medium. This allows to obtain detailed predictions on the behavior of the atomic ground state coherence, which stores the quantum information and on the re-emitted field. As a result, precise values of the storage efficiency and of the memory capacity for multimode storage are given, together with a detailed optimization procedure for the memory operation. We have also shown that if backward retrieval provides a better efficiency for a single mode, in the case of spatial multimode storage it tends to limit the number of stored modes to a lower value than the forward retrieval. With the experimental developments of short pulse storage and fast

memory registers, our model provides a reliable method to optimize the experimental conditions.

## VI. ACKNOWLEDGEMENTS

We thank Ivan Sokolov and Denis Vasilyev for the interesting discussion and remarks. The study was performed within the framework of the Russian-French Cooperation Program "Lasers and Advanced Optical Information Technologies", of the European Project HIDEAS (grant No. 221906) and of the Ile de France programme IFRAF. O.M. acknowledges the support of IFRAF. A.B. is a member of the Institut Universitaire de France. The study was also supported by RFBR (grant No. 08-02-92504).

### Appendix A: Main equations and general solutions

The light matter interaction Hamiltonian for our problem can be written as

$$\begin{aligned} \hat{V} = \int dz d^2\rho [ig & \left( \hat{a}(z, \vec{\rho}, t) e^{ik_s z - i\Delta t} \hat{\sigma}_{31}(z, \vec{\rho}, t) - \right. \\ & \hat{a}^\dagger(z, \vec{\rho}, t) e^{-ik_s z + i\Delta t} \hat{\sigma}_{13}(z, \vec{\rho}, t) \Big) + \\ & i\Omega(t) e^{ik_d z - i\Delta t} \hat{\sigma}_{32}(z, \vec{\rho}, t) - \\ & \left. i\Omega^*(t) e^{-ik_d z + i\Delta t} \hat{\sigma}_{23}(z, \vec{\rho}, t) \right], \\ & \vec{\rho} = \vec{\rho}(x, y), \end{aligned} \quad (A1)$$

where  $k_s, k_d$  are wave vectors of the signal, driving waves, and the value  $\Delta$  determines the two-photon resonance

$$\Delta = \omega_s - \omega_{13} = \omega_d - \omega_{23}. \quad (A2)$$

We perform the substitutions

$$\begin{aligned} \hat{\sigma}_{13} & \rightarrow e^{ik_s z - i\Delta t} \hat{\sigma}_{13}, & \hat{\sigma}_{23} & \rightarrow e^{ik_d z - i\Delta t} \hat{\sigma}_{23}, \\ \hat{\sigma}_{12} & \rightarrow e^{-i(k_d - k_s)z} \hat{\sigma}_{12}. \end{aligned} \quad (A3)$$

Then the Heisenberg evolution equation for the atom field system can be written as

$$\left( \frac{\partial}{\partial t} + c \frac{\partial}{\partial z} - \frac{ic}{2k_s} \Delta_\perp \right) \hat{a} = -cg \hat{\sigma}_{13}, \quad (A4)$$

$$\frac{\partial}{\partial t} \hat{\sigma}_{13} = -i\Delta \hat{\sigma}_{13} + \Omega \hat{\sigma}_{12} + g \hat{a} (\hat{N}_1 - \hat{N}_3), \quad (A5)$$

$$\frac{\partial}{\partial t} \hat{\sigma}_{12} = -\Omega^* \hat{\sigma}_{13} - g \hat{a} \hat{\sigma}_{32}, \quad (A6)$$

$$\frac{\partial}{\partial t} \hat{\sigma}_{32} = i\Delta \hat{\sigma}_{32} - \Omega^* (\hat{N}_3 - \hat{N}_2) + g \hat{a}^\dagger \hat{\sigma}_{12}, \quad (A7)$$

$$\frac{\partial}{\partial t} \hat{N}_1 = -g \hat{a} \hat{\sigma}_{31} - g \hat{a}^\dagger \hat{\sigma}_{13}, \quad (A8)$$

$$\frac{\partial}{\partial t} \hat{N}_2 = -\Omega \hat{\sigma}_{32} - \Omega^* \hat{\sigma}_{23}, \quad (A9)$$

$$\frac{\partial}{\partial t} \hat{N}_3 = -\frac{\partial}{\partial t} \hat{N}_1 - \frac{\partial}{\partial t} \hat{N}_2. \quad (A10)$$

where the transverse Laplace operator reads

$$\Delta_\perp = \frac{\partial^2}{\partial x^2} + \frac{\partial^2}{\partial y^2}. \quad (A11)$$

Here we do not take into account a spontaneous emission with rate  $\gamma$  on the transition  $|3\rangle \rightarrow |1\rangle$ . This is coupled with a requirement that in our model the field pulses are very short such that the spontaneous emission has no time to introduce something to the atomic state.

By ignoring in Eqs. (A4)-(A10) the spontaneous relaxation we nevertheless survive the frequency detuning  $\Delta$ . The condition  $\Delta \gg \gamma$  usually means that we want to treat the Raman process. However for the short pulses this condition do not ensure Raman process, here Raman interaction is realized only in the case of stronger inequality:  $\Delta \gg T^{-1}$ . In this article we consider the opposite condition  $\Delta \ll T^{-1}$ , when we are under obligatory have to neglect by  $\Delta$  in Eqs. (A5) and (A7).

From Eqs. (A4)-(A10) one can obtain that the operator

$$\hat{S}(t) = \int d^3r \left( \hat{n}(\vec{r}, t)/c + \hat{N}_2(\vec{r}, t) + \hat{N}_3(\vec{r}, t) \right) \quad (A12)$$

survives in time. Here  $\hat{n}(\vec{r}, t) = \hat{a}^\dagger(\vec{r}, t) \hat{a}(\vec{r}, t)$  is the photon number operator per second per unit area. Physically this result seems quite natural.

We assume the following conditions. All the  $N$  atoms are initially in the state  $|1\rangle$  and we assume that the signal field is much weaker than the driving field  $|\Omega|^2 \gg g^2 \langle \hat{a}^\dagger \hat{a} \rangle$ . Then most of the atoms remain in the ground state  $|1\rangle$  and in Eq. (A5) in approximation of the quasi-homogeneous medium we have a right to make a change  $(\hat{N}_1 - \hat{N}_3) \rightarrow N$  and also we can neglect the term proportional to  $\hat{\sigma}_{32}$  in Eq. (A6). Thus we obtained a reduced closed system of equations for interesting values

$$\begin{aligned} \left( \frac{1}{c} \frac{\partial}{\partial t} + \frac{\partial}{\partial z} - \frac{i}{2k_s} \Delta_\perp \right) \hat{a}(z, \vec{\rho}, t) = \\ -g \hat{\sigma}_{13}(z, \vec{\rho}, t), \end{aligned} \quad (A13)$$

$$\frac{\partial}{\partial t} \hat{\sigma}_{13}(z, \vec{\rho}, t) = gN \hat{a}(z, \vec{\rho}, t) + \Omega \hat{\sigma}_{12}(z, \vec{\rho}, t), \quad (A14)$$

$$\frac{\partial}{\partial t} \hat{\sigma}_{12}(z, \vec{\rho}, t) = -\Omega^* \hat{\sigma}_{13}(z, \vec{\rho}, t). \quad (A15)$$

We neglect the time delay linked to the pulse propagation in the atomic medium. This means if we have long enough pulses, such that  $L/c \ll T$  ( $L$  is thickness of the medium and  $T$  is the pulse duration), we can neglect the time interval between the time at which the front part of the pulse enters the medium and the time at which the front part leaves it. Formally this means we can neglect the time derivative in Eq. (A13).

Let us take the Fourier transform and next the Laplace transform of the equations according to the relations

$$\hat{F}(z, t; \vec{q}) = \frac{1}{2\pi} \int \hat{F}(z, \vec{\rho}, t) e^{-i\vec{q}\vec{\rho}} d^2\rho, \quad (A16)$$

$$\hat{F}_s(z; \vec{q}) = \int_0^\infty dt F(z, t; \vec{q}) e^{-st}. \quad (A17)$$

In the Fourier domain the equations read

$$\frac{\partial}{\partial z} \hat{a}(z, t; \vec{q}) = -g \hat{\sigma}_{13}(z, t; \vec{q}), \quad (\text{A18})$$

$$\frac{\partial}{\partial t} \hat{\sigma}_{13}(z, t; \vec{q}) = gN \hat{a}(z, t; \vec{q}) + \Omega \hat{\sigma}_{12}(z, t; \vec{q}), \quad (\text{A19})$$

$$\frac{\partial}{\partial t} \hat{\sigma}_{12}(z, t; \vec{q}) = -\Omega^* \hat{\sigma}_{13}(z, t; \vec{q}). \quad (\text{A20})$$

where we have made the changes

$$\begin{aligned} \hat{a}(z, t; \vec{q}) &\rightarrow \hat{a}(z, t; \vec{q}) e^{-iq^2 z / (2k_s)}, \\ \hat{\sigma}_{mn}(z, t; \vec{q}) &\rightarrow \hat{\sigma}_{mn}(z, t; \vec{q}) e^{-iq^2 z / (2k_s)}. \end{aligned} \quad (\text{A21})$$

In the Laplace domain the equations are written in the form

$$\frac{d\hat{a}_s(z; \vec{q})}{dz} = -g\hat{\sigma}_{13,s}(z; \vec{q}) \quad (\text{A22})$$

$$-\hat{\sigma}_{13}(z, 0; \vec{q}) + s\hat{\sigma}_{13,s}(z; \vec{q}) = gN\hat{a}_s(z; \vec{q}) + \Omega\hat{\sigma}_{12,s}(z; \vec{q}), \quad (\text{A23})$$

$$-\hat{\sigma}_{12}(z, 0; \vec{q}) + s\hat{\sigma}_{12,s}(z; \vec{q}) = -\Omega^* \hat{\sigma}_{13,s}(z; \vec{q}). \quad (\text{A24})$$

Eliminating the coherences  $\sigma_{13,s}$  and  $\sigma_{12,s}$  we obtain a differential equation for the Laplace field amplitude as :

$$\frac{d\hat{a}_s(z; \vec{q})}{dz} = -\gamma_s \hat{a}_s(z; \vec{q}) - g\hat{A}_s(z; \vec{q}), \quad (\text{A25})$$

where

$$\gamma_s = g^2 N \frac{s}{s^2 + |\Omega|^2}, \quad (\text{A26})$$

$$\hat{A}_s(z; \vec{q}) = \frac{1}{s^2 + |\Omega|^2} [\Omega \hat{\sigma}_{12}(0, z; \vec{q}) + s \hat{\sigma}_{13}(0, z; \vec{q})].$$

The solution of equation (A25) reads

$$\begin{aligned} \hat{a}_s(z; \vec{q}) &= \hat{a}_s(0; \vec{q}) e^{-\gamma_s z} - \\ &g \int_0^z dz' \hat{A}_s(z'; \vec{q}) e^{-\gamma_s(z-z')}. \end{aligned} \quad (\text{A27})$$

Taking the inverse Laplace transform we obtain the field amplitude expressed as a function of the initial conditions

$$\begin{aligned} \hat{a}(t, z; \vec{q}) &= \int_0^t dt' \hat{a}_{in}(t-t'; \vec{q}) D(t', z) - \\ &g \int_0^t dt' \int_0^z dz' \hat{A}(t-t', z-z'; \vec{q}) D(t', z'). \end{aligned} \quad (\text{A28})$$

The kernel  $D(t, z)$  is expressed from the Bessel's functions and the function  $A(t, z; \vec{q})$  reads

---


$$\begin{aligned} D(z, t) &= \delta(t) - \cos |\Omega| t \sqrt{\frac{2g^2 N z}{t}} J_1 \left( \sqrt{2g^2 N z t} \right) + \\ &+ \frac{1}{2} g^2 N z \int_0^t dt' \left[ \frac{1}{\sqrt{t'}} e^{-i|\Omega|t'} J_1 \left( \sqrt{2g^2 N z t'} \right) \right] \left[ \frac{1}{\sqrt{t-t'}} e^{i|\Omega|(t-t')} J_1 \left( \sqrt{2g^2 N z (t-t')} \right) \right], \end{aligned} \quad (\text{A29})$$

$$\hat{A}(t, z; \vec{q}) = \cos |\Omega| t \hat{\sigma}_{13}(0, z; \vec{q}) + \sin |\Omega| t \hat{\sigma}_{12}(0, z; \vec{q}). \quad (\text{A30})$$

From Eqs. (A19) and (A20) we also get explicit solutions that read

$$\hat{\sigma}_{13}(t, z; \vec{q}) = gN \int_0^t dt' \cos |\Omega|(t-t') \hat{a}(t', z; \vec{q}) + \hat{A}(t, z; \vec{q}), \quad (\text{A31})$$

$$\hat{\sigma}_{12}(t, z; \vec{q}) = e^{-i\varphi\Omega} \left[ -gN \int_0^t dt' \sin |\Omega|(t-t') \hat{a}(t', z; \vec{q}) + \hat{B}(z, t; \vec{q}) \right], \quad (\text{A32})$$

where

$$\hat{B}(z, t; \vec{q}) = -\sin |\Omega| t \hat{\sigma}_{13}(0, z; \vec{q}) + \cos |\Omega| t \hat{\sigma}_{12}(0, z; \vec{q}). \quad (\text{A33})$$

Thus we have obtained the solutions of the system of the main equations under the arbitrary initial conditions.

---

[1] M. Fleischhauer and M. D. Lukin, Phys. Rev. Lett. **84**, 5094 (2000).

[2] A.E. Kozhekin, K.Molmer, and E. Plozik, Phys. Rev. A.

- 62**, 033809 (2000).
- [3] C. Liu, Z. Dutton, C.H. Behroozi and L.V.Hau *Nature* **409**, 490, (2001).
  - [4] D. F. Philips, A. Fleischhauer, A. Mair, R. L. Walsworth, and M. D. Lukin, *Phys. Rev. Lett.* **86**, 783 (2001).
  - [5] Christoph Simon et al., *Eur. Phys. J. D* **58**, 1 (2010).
  - [6] A.I. Lvovsky, B.C. Sanders, and W. Tittel, *Nature Photonics* **3**, 706 (2009).
  - [7] T. Chanelière, D. N. Matsukevich, S. D. Jenkins, S. Y. Lan, T. A. B. Kennedy, and A. Kuzmich, *Nature (London)* **438**, 833 (2005).
  - [8] M. D. Eisaman, A. Andre, F. Massou, M. Fleischhauer, A. S. Zibrov, and M. D. Lukin, *Nature (London)* **438**, 837 (2005).
  - [9] K. S. Choi, H. Deng, J. Laurat, H. J. Kimble, *Nature* **452**, 67 (2008).
  - [10] J. Cviklinski et al., *Phys. Rev. Lett.* **101**, 133601 (2008).
  - [11] J. Appel, E. Figueroa, D. Korystov, M. Lobino and A. I. Lvovsky, *Phys. Rev. Lett.* **100**, 093602 (2008).
  - [12] K. Honda, D. Akamatsu, M. Arikawa, Y. Yokoi, K. Akiba, S. Nagatsuka, T. Tanimura, A. Furusawa and M. Kozuma, *Phys. Rev. Lett.* **100**, 093601 (2008).
  - [13] C. Clausen, I. Usmani, F. Bussi eres, N. Sangouard, M. Afzelius, H. de Riedmatten, and N. Gisin, *Nature* **469**, 508 (2011).
  - [14] E. Saglamyurek, N. Sinclair, J. Jin, J.A. Slater, D. Oblak, F. Bussi eres, M. George, R. Ricken, W. Sohler, W. Tittel, **469**, 512 (2011).
  - [15] Alexey V. Gorshkov, Axel Andr e, Mikhail D. Lukin, and Anders S. Sorensen, *Phys. Rev. A* **76**, 033804 (2007).
  - [16] Alexey V. Gorshkov, Axel Andr e, Mikhail D. Lukin, and Anders S. Sorensen, *Phys. Rev. A* **76**, 033805, (2007).
  - [17] Alexey V. Gorshkov, Axel Andr e, Mikhail D. Lukin, and Anders S. Sorensen, *Phys. Rev. A* **76**, 033806 (2007).
  - [18] Alexey V. Gorshkov, Tommaso Calarco, Mikhail D. Lukin, and Anders S. Sorensen, *Phys. Rev. A* **77**, 043806 (2008).
  - [19] K. Hammerer, A.S. Sorensen and E.S. Polzik, *Rev. Mod. Phys.* **82**, 1041 (2010).
  - [20] Q. Y. He, M. D. Reid, E. Giacobino, J. Cviklinski, and P. D Drummond "Dynamical oscillator-cavity model for quantum memories" *Phys. Rev. A* **79**, 022310 (2009)
  - [21] O.S. Mishina, D.V. Kupriyanov, J.H. M ller, E.S. Polzik, *Phys. Rev. A* **75**, 042326 (2007).
  - [22] J.-L. Le Gou et, P. R. Berman, *Phys. Rev. A* **80**, 012320 (2009)
  - [23] J. Nunn, I. A. Walmsley, M.G. Raymer, K. Surmacz, F.C. Waldermann, Z. Wang, and D. Jaksch, *Phys. Rev. A* **75**, 011401 (2007).
  - [24] S.A. Moiseev, S. Kr ll, *Phys. Rev. Lett.* **87**, 173601 (2001)
  - [25] G. H tet, J. J. Longdell, A. L. Alexander, P. K. Lam, and M. J. Sellars, *Phys. Rev. Lett.* **100**, 023601 (2008).
  - [26] G. H tet, J. J. Longdell, M. J. Sellars, P. K. Lam, and B. C. Buchler, *Phys. Rev. Lett.* **101**, 203601 (2008).
  - [27] J. Nunn, K. Reim, K. C. Lee, V. O. Lorenz, B. J. Sussman, I. A. Walmsley, and D. Jaksch, *Phys. Rev. Lett.* **101**, 260502 (2008).
  - [28] M. Afzelius, C. Simon, H. de Riedmatten, and N. Gisin, *Phys. Rev. A* **79**, 052329 (2009)
  - [29] G. H tet, M. Hosseini, B.M. Sparkes, D. Oblak, P.K. Lam, B.C. Buchler, *Opt. Lett.* **33**, 2323 (2008).
  - [30] K. F. Reim, J. Nunn, V. O. Lorenz, B. J. Sussman, K. C. Lee, N. K. Langford, D. Jaksch, I. A. Walmsley, *Nature Photonics* **4**, 218-221 (2010).
  - [31] M. Hosseini, B. M. Sparkes, G. Campbell, P. K. Lam and B. C. Buchler, *arXiv:1009.0567* (2010).
  - [32] M. P. Hedges, J. J. Longdell, Y. Li, M. J. Sellars, *Nature* **465**, 1052 (2010)
  - [33] H. de Riedmatten, M. Afzelius, M. U. Staudt, C. Simon, N. Gisin, *Nature* **456**, 773 (2008)
  - [34] D. V. Vasilyev, I. V. Sokolov, E. S. Polzik, *Phys. Rev. A* **77**, 020302 (2008).
  - [35] Denis V. Vasilyev, Ivan V. Sokolov, and Eugene S. Polzik, *Phys. Rev. A* **81**, 020302 (2010).
  - [36] M. Shuker, O. Firstenberg, R. Pugatch, A. Ron, and N. Davidson, *Phys. Rev. Lett.* **100**, 223601 (2008).
  - [37] A. Dantan, A. Bramati, and M. Pinard, *Phys. Rev. A* **71**, 043801 (2005).
  - [38] M.D. Crisp *Phys. Rev. A* **1**, 1604 (1970)
  - [39] Alexey V. Gorshkov, Axel Andr e, Michael Fleischhauer, Anders S. Sorensen and Mikhail D. Lukin, *Phys. Rev. Lett.* **98**, 123601 (2007)
  - [40] Irina Novikova, Alexey V. Gorshkov, David F. Phillips, Anders S. Sorensen, Mikhail D. Lukin, and Ronald L. Walsworth, *Phys. Rev. Lett.* **98**, 243602 (2007)
  - [41] K. Hammerer, M. M. Wolf, E. S. Polzik and J. I. Cirac, *Phys. Rev. Lett.* **94**, 150503 (2005).
  - [42] A. S. Sheremet, L. V. Gerasimov, I. M. Sokolov, D. V. Kupriyanov, O. S. Mishina, E. Giacobino, and J. Laurat, *Phys. Rev. A* **82**, 033838 (2010).